Journal of Magnetism and Magnetic Materials 557 (2022) 169473

Contents lists available at ScienceDirect

Journal of Magnetism and Magnetic Materials

journal homepage: www.elsevier.com/locate/jmmm

Research article

Effect of magnetic phase fluctuation on magnetic and magnetocaloric properties of polycrystalline $(Nd_{0.5}Sm_{0.5})_{0.5}(Sr_{0.75}Ba_{0.25})_{0.5}$ MnO_3 compound

Soma Chatterjee [a], Kalipada Das [b,*], I. Das [a]

[a] CMP Division, Saha Institute of Nuclear Physics, HBNI, AF-Bidhannagar, Kolkata 700064, India
[b] Department of physics, Seth Anandram Jaipuria College, 10-Raja Nabakrishna Street, Kolkata 700005, India

ARTICLE INFO

Keywords:
Magnetocaloric effect
Manganite
Exchange bias

ABSTRACT

The magnetic, magnetocaloric and exchange bias properties have been studied for the polycrystalline $(Nd_{0.5}Sm_{0.5})_{0.5}(Sr_{0.75}Ba_{0.25})_{0.5}MnO_3$ compound. At low temperature, antiferromagnetic counterpart of this phase separated compound transforms into ferromagnetic via a field induced metamagnetic transition. The absence of the exchange bias effect may be ascribed by the random spin freezing and existence of the paramagnetic phase even in the presence of a cooling magnetic field. Depending upon the value of the cooling field, the coercivity changes significantly. This feature may be associated with the magnetic randomness of the sample. Magnetocaloric effect calculated from M–H data (collected from different measurement protocols) indicate the remarkable modification of the ground state configuration due to magnetic field cycling. The protocol dependence MCE was explained by the field and temperature induced magnetic phase fluctuation.

1. Introduction

In doped perovskite manganites having general formula $RE_{1-x}B_xMnO_3$ (RE-trivalent and B-bivalent ions), the colossal magnetoresistance (CMR) effect is one of the most intriguing phenomena [1–6]. There are several reports published in the last two decades regarding the CMR effect and some related properties in doped perovskite compounds [1–5,7–9]. The striking correlation between the charge, spin and lattice degrees of freedom was found in these intrinsically phase-separated compounds [9–13]. In the context of the CMR effect, phase separation is considered as the key role [6,14]. In 1994, Jin et al. reported the CMR effect in doped perovskite manganite system due to the suppression of the magnetic randomness in the presence of a magnetic field near to the Curie temperature [3]. After this revolutionary work, several systematic studies have been carried out for different doped compounds having complex magnetic ground states [7, 14–17]. Except CMR effect, magnetic phase fluctuation also played vital role in other magnetic properties namely magnetocaloric effect, exchange bias, coercive fields, remanent magnetization etc. [7,8,15, 16,18]. Magnetocaloric effect is directly related with the suppression of magnetic randomness for a compound in presence of an external magnetic field. Hence, it is quite obvious to have a striking correlation between the phase fluctuation and magnetic entropy change of the system. In context to the magnetocaloric effect, it is important to mention that it can be treated as a sensitive (compared to direct magnetization measurements) tool to detect any feeble modification in magnetic state [17,19,20].

For phase separated magnetic compounds, another interesting property is exchange bias effect. Exchange bias effect (asymmetry in Magnetization vs. magnetic field loop) arises due to the unidirectional interfacial spin freezing between different types of magnetic domain [21,22]. In general, for polycrystalline compounds, random spin freezing occurs due to the absence of magnetic field during cooling. However, in the presence of external magnetic field during cooling, the directional spin freezing (exchange bias) appears and it also modifies the coercive fields of the materials [21,22]. Previously, the several physical properties of numerous quenched disordered phase separated samples having bi-critical point were reported elaborately [23,24]. In the manganite family, $(Sm_{1-x}Gd_x)_{0.55}Sr_{0.45}MnO_3$, $(Nd_{0.5}Sm_{0.5})_{0.5}Sr_{0.5}MnO_3$ and $(Nd_{0.5}Sm_{0.5})_{0.55}Sr_{0.45}MnO_3$ are very well studied compounds [25–28]. The origin of the bi-criticality of such compounds was explored considering the interfacial effect developed between different magnetic sub-domains [23,24]. The dominant components are generally antiferromagnetic and ferromagnetic (ordered/disordered) phases [23, 24,29]. The phase proportions in doped perovskite magnetic materials are also influenced by the A-site cation radius (electronic bandwidth) [4,24]. To study the effect of external magnetic field and temperature on the modification of the quenched disordered magnetic state with random fluctuation, we have selected the polycrystalline

* Corresponding author.
E-mail address: kalipadadasphysics@gmail.com (K. Das).

https://doi.org/10.1016/j.jmmm.2022.169473
Received 3 January 2022; Received in revised form 21 April 2022; Accepted 11 May 2022
Available online 18 May 2022

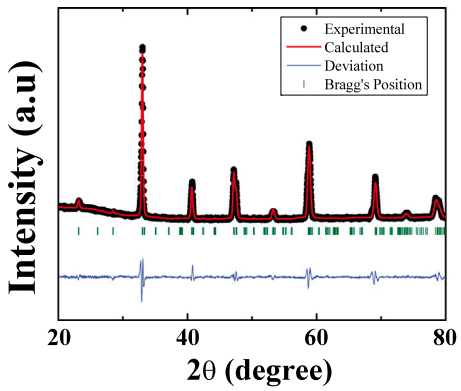

Fig. 1. Room temperature x-ray diffraction pattern (along with rietveld profile fitting) for $(Nd_{0.5}Sm_{0.5})_{0.5}(Sr_{0.75}Ba_{0.25})_{0.5}MnO_3$ compound.

$(Nd_{0.5}Sm_{0.5})_{0.5}(Sr_{0.75}Ba_{0.25})_{0.5}MnO_3$ compound having a prominent ferromagnetic phase fraction at low temperature region. The previous studies on similar compounds (near to the bi-critical region) indicate that the magnetic phase fraction and related physical properties were modified dramatically due to the influence of the external magnetic field and temperature [26–28].

In our present study, at the low temperature region, a phase-separated state is stabilized. Moreover, due to the magnetic field cycling, the proportions of different phases and related physical properties have been changed markedly. Astonishingly it should also be mentioned that exchange bias phenomena is absent for this compound. However, the change of the coercivity was observed depending upon the cooling magnetic field. Magnetocaloric effect studies, calculated from magnetization and demagnetization data indicate the distinct nature. Such features were analyzed by considering the field cycling induced modification of the different competing magnetic phases.

2. Sample preparation, characterizations and measurements

Polycrystalline $(Nd_{0.5}Sm_{0.5})_{0.5}(Sr_{0.75}Ba_{0.25})_{0.5}MnO_3$ compound was prepared by well-known solid-state reaction method. Highly pure (99.99%) Nd_2O_3, Sm_2O_3, $Sr(NO_3)_2$ and $BaCO_3$ were used as a starting element. At first, rare-earth oxides (Nd_2O_3 and Sm_2O_3) are pre-heated at 500 °C temperature for overnight. Then all the elemental powders are mixed well according to their stoichiometric ratio. The well mixed powder was then heat treated at 900–1100 °C temperature for 72 h with intermediate grinding. The polycrystalline $(Nd_{0.5}Sm_{0.5})_{0.5}(Sr_{0.75}Ba_{0.25})_{0.5}MnO_3$ sample was then reground and pressed into pallets. Finally, the pallets are sintered at 1300 °C for 36 h in air.

Room temperature powder x-ray diffraction study was carried out by Rigaku TTRAX-III diffractometer using Cu-K_α radiation(λ=1.54 Å). Magnetic measurements were performed by SuperConducting Quantum Interference Device (SQUID-VSM) magnetometer.

3. Results and discussion

Room temperature x-ray diffraction (XRD) pattern indicates the chemically single-phase nature of the polycrystalline $(Nd_{0.5}Sm_{0.5})_{0.5}(Sr_{0.75}Ba_{0.25})_{0.5}MnO_3$ compound. The XRD data for our studied sample and its profile fitting by considering 'PNMA' space group symmetry is given in Fig. 1. Extracted lattice parameters for the studied compound are a=5.4434 Å, b=5.3953 Å and c= 7.7197 Å.

Magnetization as a function of temperature at different constant magnetic fields in three different protocols — ZFCW (Zero Field Cooled Warming), FCC (Field Cooled Cooling) and FCW (Field Cooled Warming) is shown in Fig. 2. A prominent bifurcation was present between ZFCW and FCC/FCW magnetization data at H = 500 Oe external magnetic field (displayed in Fig. 2(a)). The nature of magnetization curve indicates about the presence of two clear transitions at T~150 K (shallow hump) and at T~50 K (sharp rise). Inset of Fig. 2(a) shows the variation of dM/dT with temperature T, Where M represents the FCW magnetization data at H = 500 Oe. The inset figure manifests a peak near T~150 K (correspond to antiferromagnetic phase) and a deep at T~50 K (corresponds to ferromagnetic phase). The weak response of the antiferromagnetic transition becomes more prominent in the presence of the higher value of magnetic field (shown in fig Fig. 2(b) and its inset). For more higher field values (H = 40 kOe and H = 70 kOe) the antiferromagnetic signature was absent and for H>40 kOe only ferromagnetic states are observed for this compound (shown in Fig. 2(c)). We can expect there may be a metamagnetic transition where antiferromagnetic phase transformed into ferromagnetic phases and a critical field should also present for this compound. At very low temperature region the upturn nature of magnetization may be associated with the influence of rare earth (Nd, Sm) ions. Isothermal magnetization as a function of external magnetic field at T = 2 K is given in Fig. 3(a). Here metamagnetic transition occurred near about 20 kOe external magnetic field and hysteretic nature was also observed for field cycling. To show the hysteresis nature, enlarged view of the M–H loop at the low field region is given in inset of Fig. 3(a). The magnetic field value required for metamagnetic transition (H_c) is sensitive to temperature. For the sake of clarity some selected field dependent magnetization measured at different high temperature is shown in Fig. 3(b). As the phase separated system shows exchange bias effect, we have recorded magnetization as a function of external magnetic field for some selected cooling field values at constant temperature T=2 K (shown in Fig. 4(a)). Astonishingly, exchange bias effect was absent for our studied sample. Fig. 4(b) shows that the value of exchange bias field is near about zero for all the cooling field values. However, the coercive field is changed with respect to the cooling magnetic field. The variation of coercive field as a function of cooling field is shown in Fig. 4(c). The nature of coercive field shows constant value for $H_{max}<H_c$ and then it decreases with an increasing cooling field ($H_{max}>H_c$).

Magnetocaloric effect is the variation of temperature as a function of external magnetic field under adiabatic conditions. It can also be defined as magnetic entropy change under isothermal magnetization (Demagnetization) [30]. Magnetic entropy change can be treated as a powerful tool to understand the complex magnetic ground state of materials. The magnetic entropy change was determined by using Maxwell thermodynamic relation.

$$\Delta S = \int_0^H (\partial M/\partial T) dH \quad (1)$$

For the phase separated compounds, response of different phases is very much sensitive with external magnetic field values and on its history. previously it is well documented about the measurement protocol dependency of magnetocaloric properties [14,31]. As mention earlier from the several dc magnetization measurement, the studied compound exhibits rich magnetic properties depending upon the magnetic field values and history of it.

To elucidate this fact, we have plotted the magnetic isotherm at T = 2 K (sample was cooled down in the absence of magnetic field(ZFC) and in the presence of 70 kOe magnetic field (H_c)) in the inset of Fig. 6(a). The difference between saturation magnetization of two protocols indicate that 70 kOe field is not sufficient to transform the sample fully ferromagnetic (although the ferromagnetic state is mostly dominant in nature).

Considering those facts we have estimated the magnetocaloric responses of the compound from two different set of magnetic isotherms. Magnetic entropy change was calculated from magnetic isotherms (M–H data) when the sample was subjected under 70 kOe external magnetic field. At first magnetization was measured during the increase of magnetic field from 0 to 70 kOe and then the sample was demagnetized

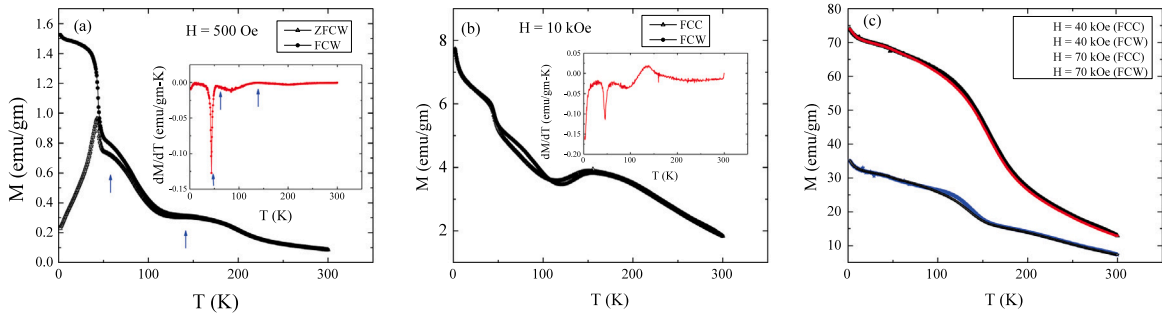

Fig. 2. (a) ZFCW and FCW magnetization as a function of temperature at H = 500 Oe magnetic field. Temperature dependence FCC and FCW magnetization is shown for (b) H = 10 kOe and (c) H = 40 kOe and H = 70 kOe. Inset of fig- (a) and (b) represents dM/dT as a function of temperature T, where M is taken from FCW data.

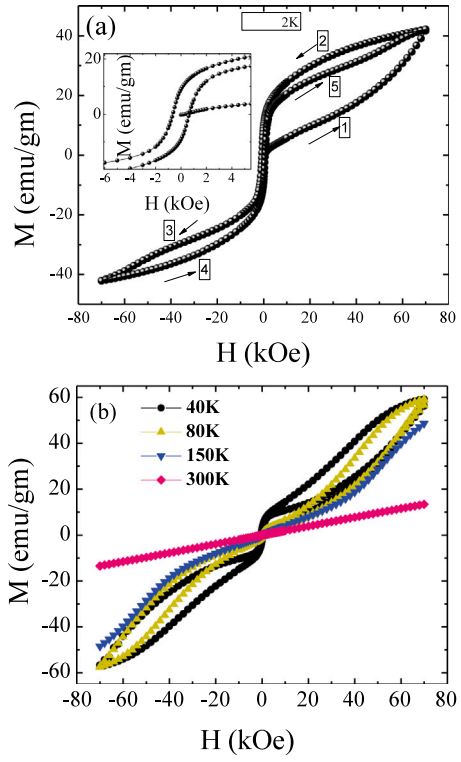

Fig. 3. (a) magnetization as a function of the external magnetic field at 2 K temperature. Inset of fig(a) shows the enlarged view of M(H) at the low field region (b) variation of magnetization with magnetic field at some selected temperature.

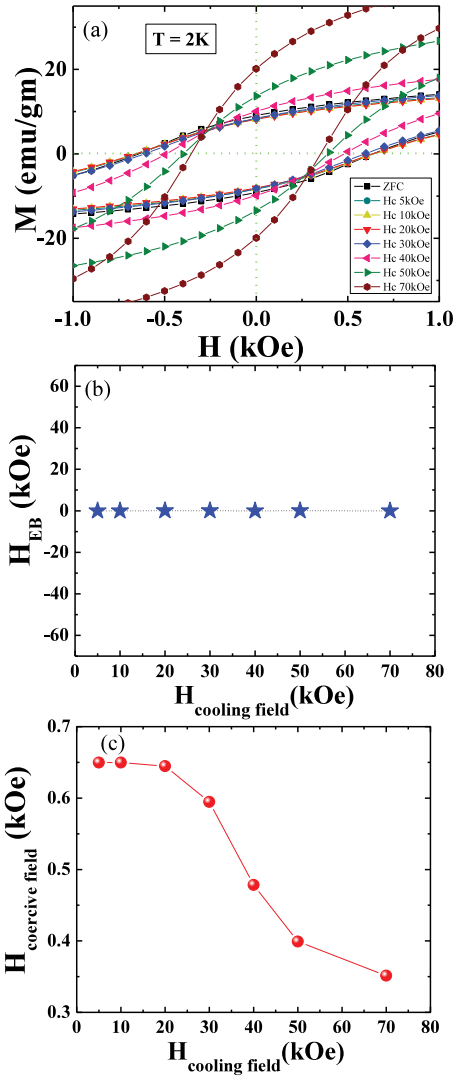

Fig. 4. (a) magnetization as a function of magnetic field at 2 K temperature for some selected cooling field. (b) and (c) represents cooling field dependent exchange bias field and coercive field respectively.

by reducing the external magnetic field from 70 to 0 kOe. Magnetic isotherms during magnetization and demagnetization at some selected particular temperatures are shown in Fig. 5. Temperature dependent magnetocaloric effect (calculation from magnetization) (Fig. 6(a)) indicate two distinct features ($H>H_c$ and $H<H_c$) depending upon the magnetic field. For small value of the magnetic field, the inherent ground state nature of the compound is prominent. As observed from the DC magnetization data, the ferromagnetic signature (T~140 K) is also clearly visible in its magnetocaloric response. With further lowering the temperature (T~50 K) the peak in MCE manifests the ferromagnetic transition of the compound. At very low temperature region the antiferromagnetic like signature appears probably due to kinetically arrested phase and short-range antiferromagnetic correlation developed among the uncompensated surface spins. However, for higher field values ($H>H_c$), $-\Delta S(T)$ at T~140 K steeply increases due to field induced phase transformation (AFM to FM). The remaining features are almost unchanged as observed for the low field region. The positive and negative sign of $-\Delta S(T)$ can probe the nature of magnetic state. Generally, In the $-\Delta S(T)$ curve a peak appears for ferromagnetic system and a positive to negative smooth crossover appears for antiferromagnetic system.

In contrast to that, the magnetocaloric response exhibits significantly different in nature when it was calculated from demagnetization data (Fig. 6(b)). Here, the predominant nature of ferromagnetic

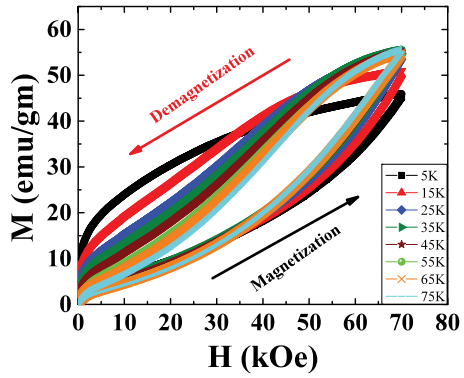

Fig. 5. Isothermal M–H curves (during magnetization and demagnetization) at some selected temperature.

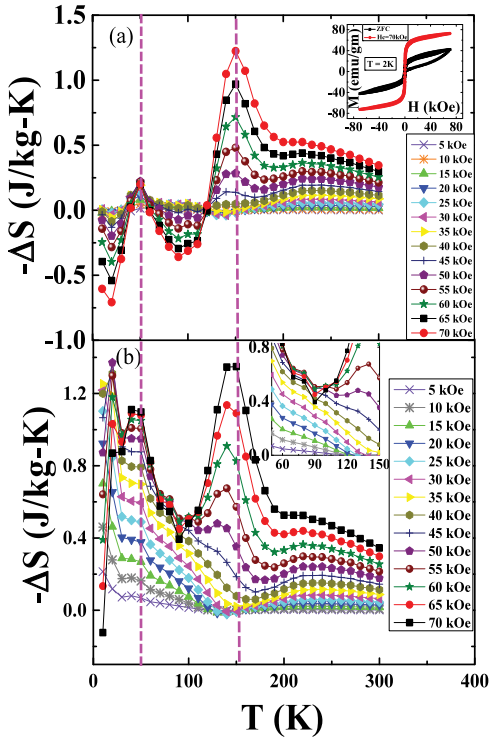

Fig. 6. (a) and (b) represents the variation of magnetic entropy change with temperature at some selected external magnetic field during magnetization and demagnetization respectively.

signature is observed throughout the whole temperature range. The antiferromagnetic like signature in the low temperature region is fully transformed into ferromagnetic counterpart. However, at T~140 K, $-\Delta S(T)$ curve shows a very small negative valued signature (corresponds to the presence of antiferromagnetic phase) for low the field region. Although the ferromagnetic counterpart is prominent for high field region, antiferromagnetic signature is also clear in view from careful observation (lowering of $-\Delta S(T)$ curve towards the zero-value shown in the inset of Fig. 6(b)). To extract the more details information about the ground state of the sample and its modification with external magnetic field, we have plotted $-\Delta S$ as a function of the external magnetic field at several specified temperatures. The calculated $-\Delta S(H)$ curves (calculated from M–H data during magnetization) at different temperature implies distinct features. For T=100 K, $-\Delta S(H)$ exhibits a positive value for H< 45 kOe. However above 45 kOe it shows a negative value. Such crossover might be ascribed as the existence

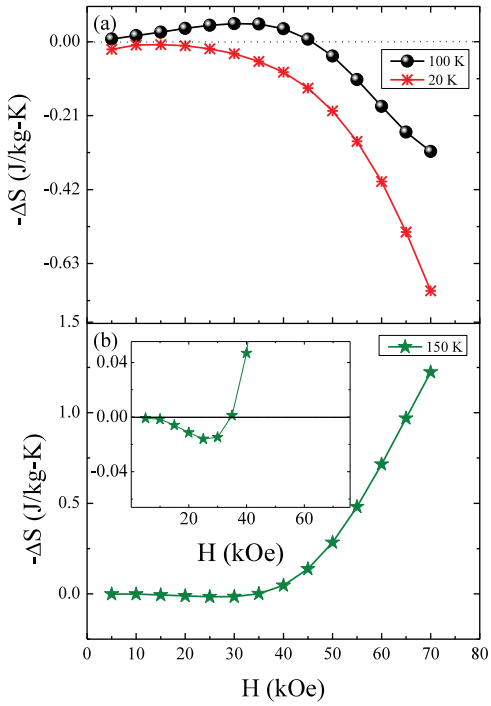

Fig. 7. Magnetic entropy change as a function of external magnetic field at (a) T=20 K, 100 K and (b) 150 K during magnetization. Inset of fig-(b) shows the external view of $-\Delta S(H)$ at low field region.

of the phase coexistence of the compound. At very low temperature region (T=20 K) the antiferromagnetic response was observed for the whole field region (Fig. 7(a)). Similarly, for T=150 K the antiferromagnetic signature of the ground state is manifested by the negative value of $-\Delta S(H)$ upto H~30 kOe. Above 30 kOe magnetic field, the ferromagnetic response become dominant due to metamagnetic transition (positive value of $-\Delta S(H)$ (Fig. 7(b)). To distinguish between the magnetic ground state before and after magnetic field cycling, we have again plotted the variation of $-\Delta S$ with H (where $-\Delta S$ have been calculated from the M–H data during demagnetization of the sample). In contrast to the previous one, at T=20 K and 100 K the dominant ferromagnetic nature was found (Fig. 8(a)). However, at T=150 K antiferromagnetic (negative $-\Delta S$) to ferromagnetic (positive $-\Delta S$) transition was found due to increase of the magnetic field (Fig. 8b).

To collect all the information regarding the magnetic ground state and its modifications, study of magnetic phase diagram is very powerful technique [14]. Especially for the compound having multiple phase transition, MCE can be treated as a powerful tool to construct the complete phase diagram [14]. In our studied sample we have constructed a magnetic phase diagram using magnetization and magnetocaloric effect (which is given in Fig. 9). The signature of the several phase transitions (temperature and field induced) are clearly visible by the phase boundary lines.

From the dc magnetization and magnetocaloric effect study we have observed that at the low field region antiferromagnetic state persists and at low field, low temperature region disordered magnetic state coexist with antiferromagnetic state. Near about H = 10–20 kOe, the disordered spins are transformed into ferromagnetic (denoted by FM(2)). For T>50k and H>10 kOe, ferromagnetic domains (denoted by FM(1)) appears along with antiferromagnetic phase due to phase transformation (AFM-FM or PM–FM). For H>60 kOe, ferromagnetic state is mostly dominating as maximum spins are aligned along the field direction and for T>160 K paramagnetic (PM) region exist. Magnetization and magnetocaloric effect study also reveals that antiferromagnetic and ferromagnetic phases are coexisted (at the low temperature region)

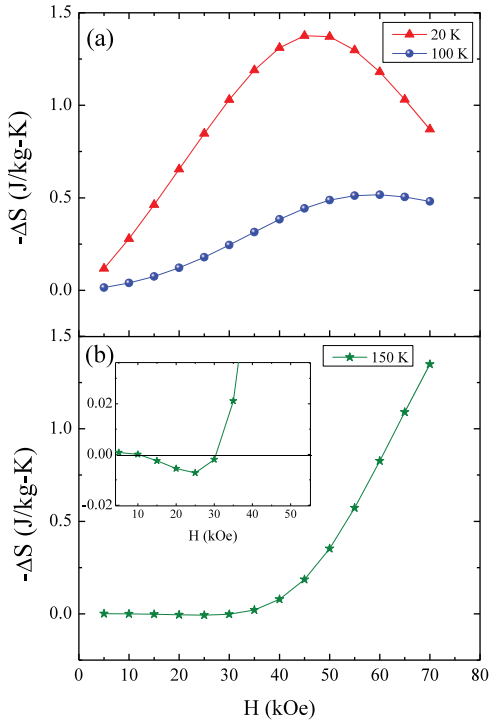

Fig. 8. Variation of magnetic entropy change with external magnetic field at (a) T=20 K, 100 K and (b) 150 K during demagnetization. Inset of fig (b) represents the enlarge view of $-\Delta S(H)$ at low field region.

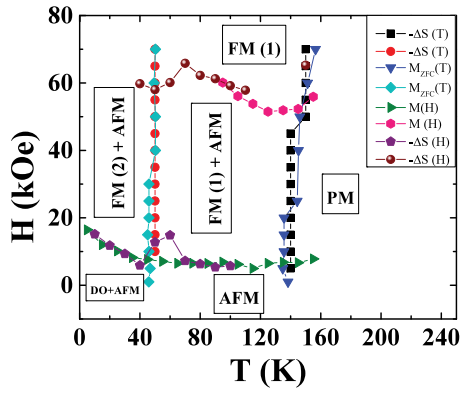

Fig. 9. Construction of magnetic phase diagram for polycrystalline $(Nd_{0.5}Sm_{0.5})_{0.5}(Sr_{0.75}Ba_{0.25})_{0.5}MnO_3$ using magnetization and magnetocaloric effect. Where AFM—antiferromagnetic, FM—ferromagnetic, DO—disordered magnetic state, PM—paramagnetic.

within the sample having different ordering temperature. Moreover, quite different nature was found for interfacial magnetic spins. The magnetic field cycling (at $T = 2$ K) influenced the interfacial spins markedly.

Considering all those facts the magnetic ground state of this compound is shown schematically in Fig. 10(a) and (b) for before and after magnetic field cycling respectively. After field cycling some of the antiferromagnetic domains transformed into ferromagnetic domains. However, at the low temperature, some remaining antiferromagnetic domains coexist with ferromagnetic phases (in the absence of a magnetic field).

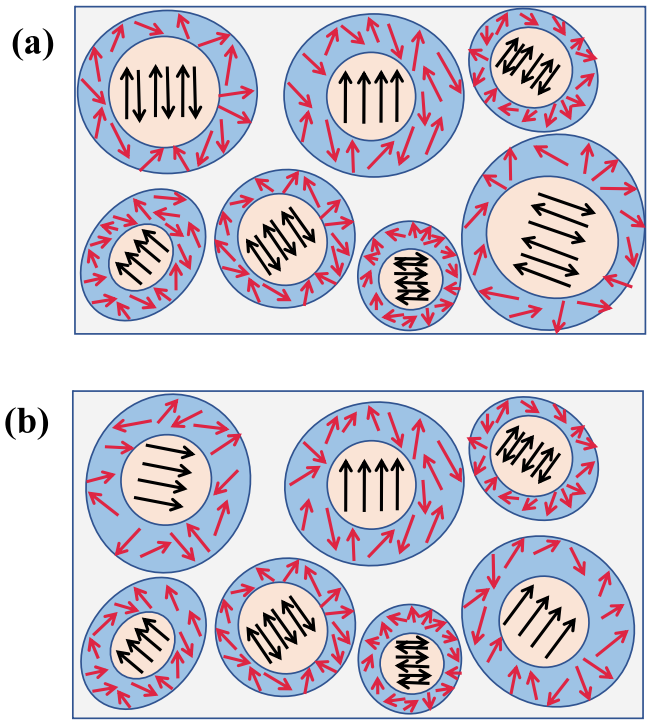

Fig. 10. (a) and (b) represents the schematic diagram before and after magnetic field cycling respectively.

4. Conclusions

In a nutshell, different magnetic properties of polycrystalline $(Nd_{0.5}Sm_{0.5})_{0.5}(Sr_{0.75}Ba_{0.25})_{0.5}MnO_3$ compound have been presented. Our experimental results indicate that for this phase separated sample the exchange bias is absent even at the low temperature region, possibly due to random spin freezing and the coexisting paramagnetic phase. However, the coercivity and the magnetic phase fraction is very much sensible on the external magnetic field. In addition, the calculated magnetocaloric effect in different protocols (during magnetization and during demagnetization) indicate the significant change of magnetic ground state for this compound.

Declaration of competing interest

The authors declare that they have no known competing financial interests or personal relationships that could have appeared to influence the work reported in this paper.

Acknowledgment

The work was supported by the Department of Atomic Energy (DAE), Govt. of India.

References

[1] J.B. Goodenough, Phys. Rev. 100 (1955) 564.
[2] E.O. Wollan, W.C. Koehler, Phys. Rev. 100 (1955) 545.
[3] S. Jin, T.H. Tiefel, M. McCormack, R.A. Fastnacht, R. Ramesh, L.H. Chen, Science 264 (1994) 413.
[4] E. Dagotto, Nanoscale phase separation and colossal magnetoresistance (springer series in solid state sciences vol 136) (berlin: Springer) and references therein, 2002.
[5] C.H. Chen, S.-W. Cheong, Phys. Rev. Lett. 76 (1996) 4042.
[6] Y. Tokura, Colossal Magnetoresistive Oxides, Gordon and Breach Science Publishers, The Netherlands, 2000.
[7] N.S. Bingham, P. Lampen, M.H. Phan, T.D. Hoang, H.D. Chinh, C.L. Zhang, S. W.Cheong, H. Srikanth, Phys. Rev. B 86 (2012) 064420.

[8] P. Lampen, N.S. Bingham, M.H. Phan, H. Kim, M. Osofsky, A. Pique, T.L. Phan, S.C. Yu, H. Srikanth, Appl. Phys. Lett. 102 (2013) 062414.
[9] Y. Tokura, Rep. Progr. Phys. 69 (2006) 797.
[10] S. Dong, F. Gao, Z.Q. Wang, J.M. Liu, Z.F. Ren, Appl. Phys. Lett. 90 (2007) 082508.
[11] Y. Tomioka, A. Asamitsu, H. Kuwahara, Y. Moritomo, Y. Tokura, Phys. Rev. B 53 (1996) R1689.
[12] Y. Okimoto, Y. Tomioka, Y. Onose, Y. Otsuka, Y. Tokura, Phys. Rev. B 57 (1998) R9377.
[13] K. Das, B. Satpati, I. Das, RSC Adv. 5 (2015) 27338.
[14] E. Dagotto, T. Hotta, A. Moreo, Phys. Rep. 344 (2001) 1–153.
[15] M.H. Phan, S. Chandra, N.S. Bingham, H. Srikanth, C.L. Zhang, S.W. Cheong, T.D. Hoang, H.D. Chinh, Appl. Phys. Lett. 97 (2010) 242506.
[16] M.H. Phan, S.C. Yu, J. Magn. Magn. Mater. 308 (2007) 325.
[17] K. Das, I. Das, J. Appl. Phys. 119 (2016) 093903.
[18] P. Lampen, A. Puri, M.H. Phan, H. Srikanth, J. Alloys Compd. 512 (2012) 94–99.
[19] A.M. Tishin, Y.I. Spichkin, The Magnetocaloric Effect and Its Applications, Institute of Physics Publishing, Bristol and Philadelphia, 2003.
[20] T. Samanta, A.U. Saleheen, D.L. Lepkowski, A. Shankar, I. Dubenko, A. Quetz, M. Khan, N. Ali, S. Stadler, Phys. Rev. B 91 (2014) 064412.
[21] W.H. Meiklejohn, C.P. Bean, Phys. Rev. 102 (1956) 1413.
[22] S. Giri, M. Patra, S. Majumdar, J. Phys.: Condens. Matter 23 (2011) 073201.
[23] A.K. Pramanik, A. Banerjee, J. Phys.: Condens. Matter 20 (2008) 275207.
[24] Y. Tokura, Rep. Progr. Phys. 69 (2006) 797.
[25] B.M. Todris, E.A. Dvornikov, F.N. Bukhan'ko, V.I. Val'kov, Low Temp. Phys. 35 (2009) 10.
[26] Y. Tomioka, X.Z. Yu, T. Ito, Y. Matsui, Y. Tokura, Phys. Rev. B 80 (2009) 094406.
[27] A. Machida, Y. Moritomo, A. Nakamura, Phys. Rev. B 58 (1998) 19.
[28] N.A. Babushkina, E.A. Chistotina, A.M. Balagurov, V.Yu. Pomjakushin, O.Yu. Gorbenko, A.R. Kaul, M.S. Kartavtseva, J. Magn. Magn. Mater. 300 (2006) 114–117.
[29] T. Hotta, E. Dagotto, Phys. Rev. B 61 (2000) R11879.
[30] A. Anitha, M. Manjuladevi, R.K. Veena, V.S. Veena, S.K. Yuri, S. Sagar, J. Magn. Magn. Mater. 528 (2021) 167810.
[31] T. Paramanik, K. Das, T. Samanta, I. Das, J. Magn. Magn. Mater. 381 (2015) 168–172.